Project 007021 (ISTC Project 1914p)

Laser with Wavelength 0.589 μm ("Sodium Wavelength Laser")

Final Report

Nikolay Il'ichev, General Physics Institute, Moscow, Russia

Summary

Sodium cell is suggested to implement to stabilise generation frequency of the LiF:F_2^- laser. Initial transmission of the sodium cell, temperature and stability of temperature of the cell are estimated. Sodium cell and oven for the cell were developed, manufactured and tested.

Spectrum width and generation frequency stability that is due to LiF active element rotation and spherical aberrations of telescope elements are discussed. Calculation shows that the laser generation frequency stability it is possible to do better than 0.05 cm^{-1}.

Spectral selection and output power characteristics of LiF:F_2^- colour centres laser with rotating active element at pumping by YAG:Nd cw laser were studied experimentally. It was obtained output power 340 mW at narrow (0.1 – 0.2 cm^{-1}) spectrum width at pump power 5.6 W. Without spectral selection it was obtained about 650 mW at pump power 6.5 W.

Additional internal resonator Fabry-Perot interferometer for narrowing generation spectrum (base 1.6 mm and mirror reflectivity 70 %) was developed and tested. Spectrum width 0.03 – 0.04 cm^{-1} and frequency stability better than 0.03 cm^{-1} during 20 minutes at wavelength 1.15 μm were obtained.

REPORT DOCUMENTATION PAGE

Form Approved OMB No. 0704-0188

1. REPORT DATE *(DD-MM-YYYY)*	2. REPORT TYPE	3. DATES COVERED *(From – To)*
24-01-2002	Final Report	27-Nov-00 - 27-Nov-01

4. TITLE AND SUBTITLE

Laser with Wavelength 589 nm

5a. CONTRACT NUMBER
ISTC Registration No: 1914p

5b. GRANT NUMBER

5c. PROGRAM ELEMENT NUMBER

6. AUTHOR(S)

Professor Nikolay Ilichev

5d. PROJECT NUMBER

5d. TASK NUMBER

5e. WORK UNIT NUMBER

7. PERFORMING ORGANIZATION NAME(S) AND ADDRESS(ES)

General Physics Institute of the Russian Academy of Sciences
38 Vavilov St
Moscow 117942
Russia

8. PERFORMING ORGANIZATION REPORT NUMBER

N/A

9. SPONSORING/MONITORING AGENCY NAME(S) AND ADDRESS(ES)

EOARD
PSC 802 BOX 14
FPO 09499-0014

10. SPONSOR/MONITOR'S ACRONYM(S)

11. SPONSOR/MONITOR'S REPORT NUMBER(S)
ISTC 00-7021

12. DISTRIBUTION/AVAILABILITY STATEMENT

Approved for public release; distribution is unlimited.

13. SUPPLEMENTARY NOTES

14. ABSTRACT

This report results from a contract tasking General Physics Institute of the Russian Academy of Sciences as follows: The objective of this project is to develop a laser system based on F2- color centers in LiF crystals with frequency doubling, which produces from 10 to 40 Watts average output power radiation at 589 nm, the wavelength of the sodium fluorescence, and with the spectral width of the radiation being several hundred megahertz. It is pumped by a high power Nd:YAG laser. This is a continuation of an effort that has been going on for two years.

15. SUBJECT TERMS
EOARD, Physics, Optics

16. SECURITY CLASSIFICATION OF:			17. LIMITATION OF ABSTRACT	18, NUMBER OF PAGES	19a. NAME OF RESPONSIBLE PERSON
a. REPORT	b. ABSTRACT	c. THIS PAGE			Alexander J. Glass, Dr
UNCLAS	UNCLAS	UNCLAS	UL	27	19b. TELEPHONE NUMBER *(Include area code)* +44 (0)20 7514 4953

Contents

1. Development of spectral selection system for tuning LiF:F_2^- laser at the wavelength second harmonic of which is D_1 or D_2 line of sodium.

The main characteristics of spectral selection system of a LiF :F_2^- colour centres laser are defined by sodium absorption spectra. It is appropriate to remind of them here.

1) Wavelength of second harmonic of LiF :F_2^- output radiation has to be at 589.6 nm or 589.2 nm (D_1 and D_2 sodium lines).

2) Spectrum width of the radiation should be at least equal to Doppler width of sodium. There are a lot of papers concerning with measuring and calculation of this width at different conditions. Paper [1] is one most closely related to the problem under consideration. In this paper for example spectral width is estimated as 2 GHz at 215 K.

To meet these requirements it is necessary to have a system to control wavelength of radiation and an executive element to tune output radiation wavelength at the centre of a sodium line when there is some misalignment. Principal scheme of laser spectrum selection was suggested earlier [2]. This scheme has to be supplemented with some part that gives possibility to control exact wavelength of radiation. We suggest using sodium vapour cell as reference wavelength element.

1.1. Scheme of spectral selection system

There is principal optical scheme of the LiF :F_2^- colour centres laser with wavelength tuning in Fig. 1. Numbers denote 1 - 11 are LiF :F_2^- laser resonator elements; 1, 4, 6, and 7 are the laser resonator mirrors, 2 is rotating LiF:F_2^- colour centres active element, 3 is lens; 5 is etalon Fabry-Perot for rough wavelength tuning, 8 is optical wedge compensator, 9 and 10 are lenses of telescope; 11 – grating, 12 is mirror, 13 is SHG crystal, 14 is plate, 15 is sodium cell in oven, 16 and 17 photodiodes for measuring of incident and passed through the sodium cell radiation. Two optical wedges (8) that are rotated in opposite directions used for fine tuning of wavelength of radiation.

Sodium cell in oven (15) will serve as reference element to control wavelength of radiation. Second harmonic of the output laser radiation will pass through a sodium cell. If radiation frequency is near the centre of a sodium resonance line then change of the cell transmission will indicate that wavelength changed (if temperature of the cell is constant). Working frequency correspond to minimum transmission of the sell.

1.2. Sodium cell parameters

Here we define temperature, precision of temperature and initial transmission of the cell. To choose temperature of sodium cell it is necessary to know sodium vapour density and effective cross section of sodium transition. Saturated sodium vapour pressure as function of temperature is tabulated [3]. We have a cell with length 20 cm. There are different estimations of effective cross section σ of sodium D_2 – line transition in literature. For example in [4] effective cross section at temperature T=215 °K is $\sigma=3.0\cdot10^{-12}$ cm^2, in [1] it is $\sigma=8.8\cdot10^{-12}$ cm^2. We use these two estimations of cross section for evaluation of possible temperature range of the cell. In Fig. 2 there is transmission of our cell (length is equal to 20 cm) as function of temperature. From this picture one can see that possible temperature of cell T_c lays at the range 105 °C<T_c<125 °C. For us it is important that upper limit of the range is not high so it is technically easy to do.

Transmission $T(\nu)$ of a sodium cell depends on frequency ν near the centre of the absorption line. At fixed temperature t and at low power density probe beam level (saturation of absorption is absent) it is

$$T(\nu)=\exp(-\sigma(\nu)\cdot N(t)\cdot l), \tag{1}$$

where $\sigma(\nu)=\sigma_0\cdot\exp(-\left(\frac{\nu-\nu_0}{\Delta\nu_D}\right)^2\cdot\ln(2))$, $\Delta\nu_D$ is a Doppler D line width (HWHM), $N(t)$ is sodium vapour density, l is the cell length. If consider sodium vapour is ideal gas and use expression for sodium saturated vapour pressure [5] then we have for $N(t)$

$$N(t)=A\cdot\frac{1}{t}\cdot\exp(-\frac{\Delta H}{R\cdot t}), \tag{2}$$

where ΔH is evaporation heat (for sodium ΔH=90.1 kJ/mole [3]) and R=8.3 J/mole·K is molar gas constant, A is a constant. From (1) and (2) change of sodium cell transmission δT that is due to change of temperature δt at constant frequency is

$$\delta t=\frac{\delta T\cdot R\cdot t^2}{T\cdot\ln(\frac{1}{T})\cdot\Delta H}, \tag{3}$$

where T is transmission of sodium cell at central frequency, δT is precision of transmission measurement, t is temperature of sodium cell. For numerical estimation of this value it is necessary to know values T and δT.

Experimentally measured transmission T is ratio of two signals $T=\frac{U_{out}}{U_{in}}$, where U_{in} and U_{out} are signals from photodiodes (see Fig. 1) at input and output of sodium cell that are proportional to input and output power of radiation. Signals U_{in} and U_{out} can be measured with some precision ΔU_{in} and ΔU_{out}. For example ΔU_{in} or ΔU_{out} could not be less than digitisation step of analogue

digital converter. These values define precision of transmission measurement $\delta T = \frac{|\Delta U_{out}|}{U_{in}} + T \cdot \frac{|\Delta U_{in}|}{U_{in}}$. As $T \leq 1$ for estimation it is possible to assume that δT is equal to $\delta T \approx \frac{|\Delta U_{out}| + |\Delta U_{in}|}{U_{in}}$ and does not depend on transmission T. This value δT defines frequency range where change of frequency $\Delta\nu$ cannot be detected by our measurement system: $\delta T = T(\nu_0 + \Delta\nu) - T(\nu_0)$. Expanding in series expression (1) about ν_0 it is possible to obtain

$$\frac{\Delta\nu}{\Delta\nu_D} = \sqrt{\frac{-\delta T}{T \cdot \ln(T) \cdot \ln(2)}}. \qquad (4)$$

In Fig. 2 there is plotted $f(T, \delta T) = \frac{\Delta\nu}{\Delta\nu_D}$ as function T at δT=0.01. It possible to see from (4) that there is transmission $T_{\min}$ of sodium cell at which change of frequency due to temperature instability is minimal. This transmission is independent of δT and is $T_{\min}$=exp(-1)=0.368, and $f(T_{\min}, \delta T) \approx 2 \cdot \sqrt{\delta T}$. For T=$T_{\min}$ and δT=0.01, at $t \approx 400$ °K from (3) we obtain accuracy of temperature of sodium cell δt=0.4 °C.

1.3. LiF:F_2^- colour centres laser resonator instabilities and generation frequency

Spectral selection properties of the scheme in Fig. 1 were studied theoretically and experimentally earlier [2]. It was shown experimentally that it is possible in principle to obtain spectral width of laser radiation 0.1 cm^{-1} with the same stability. In [2] magnification of telescope was 5^x and diameter of laser radiation on grating was about 1.5 cm. Objective of our telescope has optical diameter 5 cm and grating length is 10 cm. So it is possible to obtain higher selectivity at higher magnification of the telescope with shorter eyepiece. But some problems were left out of consideration. LiF:F_2^- active element of our laser is rotated. There is an angle between axis of rotation and perpendicular to optical face of the element. This misalignment always takes place due to precision of manufacturing. There is some optical wedge in active element too. So during rotation position of optical axis of the resonator is changed. Change of optical axis position may lead to frequency shift of output laser radiation.

In Fig. 4 there is part of the LiF:F_2^- colour centres laser resonator from Fig. 1 where distances between resonator elements are designated. Numbers in Fig. 4 denotes the same elements as in Fig. 1. Mirror 4 is plane and is used to make the resonator more compact so it is not taken into consideration. Optical resonator axis position at mirror 6 depends on tilt angle of active LiF element and optical wedge in it. Mirror 6 is plane so it is possible to consider (and calculation

gives the same result) that wave front of TEM_{00} mode is plane and it is parallel to mirror plane, e.i. optical axis of the resonator is always perpendicular to the mirror 6 plane.

Let us calculate axis position at mirror 6 as function of tilt angles of LiF optical faces with respect to optical axis of resonator when these angles are zero. Extended 3x3 matrices [6] are implemented. Matrix of pass of optical ray through LiF active element is described as multiplication of three matrices $N_{out}(\theta_2)\cdot D(l_s)\cdot N_{in}(\theta_1)$, where θ_1 and θ_2 are angles between normal vector at input and output faces of LiF and resonator optical axis. Tilt of LiF active element at angle θ corresponds to $\theta_1=\theta_2=\theta$. It is possible to obtain for the matrices

$$N_{in}(\theta_1)=\begin{bmatrix}1 & 0 & 0\\ 0 & \frac{1}{n} & \theta_1\cdot(\frac{1}{n}-1)\\ 0 & 0 & 1\end{bmatrix},\ N_{out}(\theta_2)=\begin{bmatrix}1 & 0 & 0\\ 0 & n & \theta_2\cdot(n-1)\\ 0 & 0 & 1\end{bmatrix},\ D(l_s)=\begin{bmatrix}1 & l_s & 0\\ 0 & 1 & 0\\ 0 & 0 & 1\end{bmatrix},$$

n is refraction index of LiF (n=1.38 [3]), l_s is length of LiF crystal. Matrix $D(d)$ is matrix of free space with length d. Full matrix $M=\begin{bmatrix}A & B & \Delta y\\ C & D & \Delta V\\ 0 & 0 & 1\end{bmatrix}$ is obtained by multiplication of extended matrices of all resonator elements (including free spaces) on the round trip of resonator: $M = M2\cdot M1$, where

$M1 = D(l_1-\frac{l_s}{2})\cdot N_{out}(-\theta_1)\cdot D(l_s)\cdot N_{in}(-\theta_2)\cdot D(l_2-\frac{l_s}{2})\cdot F(f)\cdot D(d-l_1-l_2)\cdot F(\frac{r_2}{2})$ and

$M2 = D(d-l_1-l_2)\cdot F(f)\cdot D(l_2-\frac{l_s}{2})\cdot N_{out}(\theta_2)D(l_s)\cdot N_{in}(\theta_1)\cdot D(l_1-\frac{l_s}{2})\cdot F(\frac{r_1}{2})$. Matrices D and N were defined above and $F(f)=\begin{bmatrix}1 & 0 & 0\\ -\frac{1}{f} & 1 & 0\\ 0 & 0 & 1\end{bmatrix}$ is matrix of lens with focal length f [6]. Values l_1, l_2 and d are denoted in Fig. 4. This expression is written for the point of resonator at mirror 6.Values Δy, ΔV are due to resonator elements misalignment. In our case they all are connected with LiF active element. A, B, C, D are elements of the usual $ABCD$-matrix. Optical axis position is obtained as solution of the next equation [6]

$$\begin{bmatrix}A & B & \Delta y\\ C & D & \Delta V\\ 0 & 0 & 1\end{bmatrix}\cdot\begin{bmatrix}y_0\\ V_0\\ 1\end{bmatrix}=\begin{bmatrix}y_0\\ V_0\\ 1\end{bmatrix}, \qquad (5)$$

where y_0 and V_0 are transverse co-ordinate and angle of optical axis. At Δy=0 and ΔV=0 we have y_0=0 and V_0=0.

Up to now [2] we chose the LiF resonator configuration from the point of view of insensitivity TEM_{00} diameter inside active element to thermal lens inside this element. Now we discuss the problem of optical resonator axis position stability when LiF is rotating for different resonator configurations. We fix resonator length d=111 cm. Radius of curvature of mirror 1 is r_1=6.5 cm. Mirror 6 is plane $r_2=\infty$. At almost any position of lens 3 inside resonator there is focal length of the lens when trace of $ABCD$-matrix is zero: $A+D=0$. Calculation shows that at this condition resonator is stable if focal length of lens inside LiF is $|f_s| > 10$ cm and mode waist is in the middle of LiF. Length of our LiF is 2.8 cm. Resonator with focal length of lens 3 equal to 20 cm was tested experimentally earlier [2,7].

In Fig. 5 there is dependence of optical axis position y_0 at mirror 6 as function of focal length of lens 3. These curves were obtained as solution of equation (5) at conditions stated above. Angles θ_1 and θ_2 were 10^{-3} rad and are at least several times more then we have in experiment.

A question may arise that curve 2 seems to be mirror of 3 (Fig. 5) with respect to ordinate axis because LiF is optical wedge orientated in opposite directions for these cases. But calculation shows that if length of LiF crystal is zero (thin optical wedge) then curve 2 becomes mirror of curve 3.

During LiF rotation position of resonator optical axis changes and in turn beam at output of telescope (after lens 10, Fig. 1) changes too. Position of telescope eyepiece 9 should be aligned in the way that wave front of beam after telescope is plane. This is necessary because selective characteristics of grating are defined by an angular divergence of incident on grating radiation. Efficiency of spectrum selection depends also on quantity of radiation that is returned back into TEM_{00} – mode of laser resonator formed by mirrors 1 and 6 (see Fig. 1), e.i. mode matching is the best if the wave front is plane. Mirror 6 is situated at some distance from eyepiece and thus curvature of radiation at input of the telescope is not zero, so transverse shift of optical axis of resonator will lead to change of direction of the axis after telescope (telescope is not aligned at infinity, it make plane wave front before grating). This means that angle of incidence at the grating will be changed and thus generation frequency of the LiF:F_2^- laser will be changed too.

Frequency shift $\Delta\nu_s$ can be estimated as $\Delta\nu_s = \frac{1}{\lambda \cdot tg(\theta_0)} \cdot \frac{y_0}{C1}$, λ=1.178 μm is wavelength of generation, θ_0 is angle of incidence of central (optical axis) ray on grating: $2 \cdot \sin(\theta_0) = \lambda \cdot g$, $\frac{1}{g}$ is grating period; $C1$ is C element of $ABCD$ matrix that describes propagation of radiation from mirror 6 to point where grating is situated.

In Fig. 6 there is presented calculated generation frequency shift of LiF:F_2^- laser that is due to rotation LiF active element as function of focal length of lens 3 (Fig. 1). Value y_0 are presented in Fig. 5. Calculation conditions for these three curves are the same as for ones in Fig. 5. From Fig. 6 it is clear that the more focal length of lens 3 the less $\Delta\nu_s$. Focal length of the lens should be 20 – 60 cm to have frequency shift less then 0.05 cm^{-1}.

Generation spectrum width depends on not only characteristics of spectrum selection system but on stability of pumping laser radiation (power and divergence). Experiment shows [2, 7] that if telescope focal length of objective is 60 cm and eyepiece is 12 cm, grating has 300 grooves/mm then generation spectrum width is 0.1 cm^{-1}. It should be mentioned here that frequency stability can be improved if additional Fabry-Perot interferometer is inserted inside LiF:F_2^- laser resonator nearby interferometer 5 (Fig. 1). Base of this new interferometer we choose 0.5 cm and reflectivity of its mirrors 50 %. In this case it is possible to change place of optical wedges 8 (Fig. 1) and use them inside the resonator. Then new Fabry-Perot interferometer is placed between the wedges and rotation of them is lead to change of angle incidence of radiation at the Fabry-Perot thus changing transmission frequency. This additional interferometer will stabilise frequency of the laser radiation and make higher the system reliability. In this case grating system is served to suppress side transmission frequency resonance of the interferometer. At this stage of work it is better to have some spare reserve. It is always possible not to use it if it is not necessary.

1.4. Aberrations of telescope elements and generation spectrum

Let us consider spherical aberration of the telescope eyepiece and objective. Spherical aberration means that if optical ray that is propagates parallel to optical axis passes through a lens at some distance h from the optical axis centre then it (or its continuation) goes not to focal point but at some distance δ from optical axis at focal plane of the lens. Expression for δ when source is at infinity is [8]

$$\delta(h) = f(R_1, R_2, n_0)\cdot h^3, \tag{6}$$

where $f(R_1, R_2, n_0) = \frac{n_0^2}{4}\cdot\left[\frac{1}{R_1^2}\cdot\left[1-\frac{2\cdot(n_0^2-1)}{n_0^3}\right]+\frac{1}{R_1\cdot R_2}\cdot\left[\frac{1}{n_0^2}+\frac{2}{n_0}-2\right]+\frac{1}{R_2^2}\right]$, R_1 and R_2 are radii of curvature of lens surfaces; n_0 is index of the lens material. Division of first differential of expression (6) on focal length of objective gives change of angle of incidence $\Delta\theta$ at grating that is due optical axis shift y_0 at eyepiece. For eyepiece it is $\Delta\theta = 3\cdot f(R_1, R_2, n_0)\cdot h^2\cdot\frac{y_0}{f_t}$ where f_t is focal length of objective 10 (Fig. 1). Expression for objective we obtain if substitute h and y_0 on

h and $y_{0,1}$: $h_1 = h \cdot M$ and $y_{0,1} = y_0 \cdot M$, M is telescope magnification, R_1 and R_2 are radii for objective lens. Frequency shift that is due to spherical aberration of telescope elements and LiF rotation is $\Delta\nu_s = \frac{1}{\lambda \cdot tg(\theta_0)} \cdot \Delta\theta_1$, where $\Delta\theta_1$ is summary eyepiece and objective angle. In Fig. 7 there is $\Delta\nu_s$ as function of h. Values for calculation are: eyepiece R_1=6.24 cm R_2=∞, n_0=1.52, f_e=-12 cm; objective R_1=31.2 cm R_2=∞, n_0=1.52, f_o=60 cm; grating has 300 grooves/mm; y_0=100 μm. This calculation shows how LiF rotation and telescope alignment are connected with generation frequency stability. From Fig. 7 it is possible to see that if h<1 mm than frequency shift is less than 0.02 cm^{-1}.

2. Generation characteristics of a LiF: F_2^- laser with rotating active element

Heat removing from pumping area is important problem to be solved for development high power LiF:F_2^- colour centres laser. The importance of the problem can be seen from the fact that it is considered that heat dissipation prevents cw oscillation LiF:F_2^- laser [9]. It was suggested in [10] to implement rotating active element for effective heat removing from pumping area of LiF:F_2^- laser and cw laser generation with rotating LiF crystal was obtained. Spectral selection and output power characteristics of LiF:F_2^- colour centres laser with rotating active element at pumping by YAG:Nd cw laser were studied experimentally and results are presented below.

2.1. Experimental setup

There is experimental setup for measuring parameters of LiF:F_2^- laser with rotating active element in Fig.8. 1 – 9 are LiF:F_2^- laser resonator elements; 1 - mirror reflectivity R at wavelength 1.064 mkm R(1.064 mkm)≈5%, R(1.178 mkm)=98%, radius of curvature 6.5 cm; 2 – rotating LiF:F_2^- colour centres active element, length 30 mm, transmission at 1.064 mkm 50%; 3 – lens with focal length 20 cm; 4 – flat mirror R(1.064 - 1.178 mkm)≈100%; 5 – flat mirror R(1.15 - 1.178 mkm)≈70%; 6 – flat output mirror, mirrors with different reflectivity were used; 7 , 8 – lenses of telescope, magnification 5^x ; 9 – grating with 300 grooves per mm; 10 – grating with 600 grooves per mm; 11 – screen to eliminate radiation at 1.064 mkm; 12 – power meter. Distances: L(1–2)=5 cm, L(1–3)=32.8 cm, L(1-4)=72.7 cm, L(4-5)=37.8, L(1–5)=109.9 cm, L(5-6)=40.5 cm, L(6-7)=19.1 cm, L(6-8)=67.2 cm, L(6-9)=69.2 cm, L(5-9)=109.7 cm. It was possible to move the mirror 5 in the direction of optical axis of the laser resonator to make optical distances L(1-5) and L(5-9) equal each other. Telescope 7, 8 and grating 9 were implemented as spectral selection elements. Selected by the grating part of spectrum was

reflected back into the resonator 1 – 5 and influenced on the laser radiation spectrum. Spectral characteristics of this spectrum selector were discussed earlier [10]. Mirror 6 was output mirror and output radiation was propagated in the direction as it is pointed out by arrow in Fig. 8.

2.2. Input - output power characteristics of the LiF:F_2^- laser

There is scheme of LiF:F_2^- laser output power measurement in Fig. 8. Grating 10 was implemented to separate pump and generation radiation. Reflectivity of grating 10 was measured at wavelength 1.064 mkm R_g=80% and it was assumed that at wavelength of generation reflectivity was the same.

There is output power vs input power in Fig. 9 at different reflectivity of mirror 6. Pump power was measured at input face of LiF:F_2^- crystal. Slope efficiency is 14.8% (curve 1), 11.6% (2), 4.8% (3). These curves have different spectrum of radiation and this question is discussed below. From this picture it is possible to see that the lower reflectivity of mirror 6 the higher efficiency. This dependence is due to special feature of the laser scheme because part of laser radiation reflected by grating 9 (see Fig. 8) passes through mirror 6 and may be counted as loss. But output spectrum depends on reflectivity of this mirror too and the lower reflectivity the less efficient is spectral selection. It is important to know spectral characteristics of laser vs reflectivity of mirror 6.

2.3. LiF:F_2^- laser radiation spectrum

There is scheme of measurement of output radiation spectrum in Fig. 10. The LiF:F_2^- laser output radiation was reflected by grating 3 (600 groove per mm) in the first order and focused by lens on CCD camera matrix. This scheme has low resolution (approximately 5 cm^{-1}) and choice of the scheme was due to peculiarity of the spectrum. If reflectivity of mirror 6 is less than 40% the spectrum has shape of wide (about 150 cm^{-1}) background and narrow (0.1 - 0.2 cm^{-1}) peak. At reflectivity of mirror 6 higher 40 % spectrum is narrow (0.1 – 0.2 cm^{-1}) and background is not detectable. There are spectra of laser radiation in Fig. 11 at reflectivity of mirror 6 25%. Curves illustrate case of narrow (1) and wide (2) spectrum. In the former case selection scheme is switched off by opaque screen installed inside the LiF:F_2^- laser resonator between mirror 6 and telescope (see Fig. 8). Output power is the same for these two cases. Scale for curve 2 Fig. 11 is 20 times more than for curve 1. Background for curve 1 is screened by noise so this scheme is not good for quantitative estimation of power in narrow and wide parts of spectrum.

In Fig. 12 there is layout of measurement of ratio power in narrow spectrum to total power. This scheme is like the one in Fig. 10 but instead CCD – camera there is power meter 1 and at

focal plane of lens 2 there is slit 4. Width of the slit was chosen to allow the narrow spectral peak to pass through it without attenuation. It was measured power passed through the slit and total power of generation when the slit was removed.

During this experiment reflectivity R of mirror 6 was taken 40% and between this mirror and the telescope lens 7 (see Fig. 8) was inserted attenuator with transmission T. This case is the same as we use mirror with efficient reflectivity $R_{\text{eff}}=T^2R$. There is ratio $F=P_w/P_t$ in Fig. 13. P_t is total power and P_w is wide spectrum width power. There was mirror with reflectivity 25% in our disposition and it was compared values of F obtained with attenuator and with this mirror. These data were close to each other. Wide spectrum width power can be considered as loss so it is possible to write $P_n= P_0(1-R)(1-F)$, P_n is narrow spectrum width power, P_0 is total generation power propagating from mirror 5 to mirror 6. If we define efficiency of spectral selection scheme (*ESS*) as $ESS=P_n/P_0$ then we have $ESS=(1-R)(1-F)$. Generally speaking P_0 depends on reflectivity of mirror 6, but we neglect interference between of grating 9 and mirror 5 (see Fig. 8). This is possible to do because threshold only slightly depends on reflectivity of mirror 6 (see Fig. 9) and in turn this indicates that interference is minor effect at our conditions. There is *ESS* as function of R_{eff} in Fig. 14. It is possible to see that optimum reflectivity of mirror 6 at our conditions lies at range 25% - 33%.

Curve 2 in Fig. 9 was obtained at reflectivity of mirror 6 25%. Having in mind that at narrow part of spectrum there was 85% (see Fig. 13) we can say that slope efficiency at narrow spectrum width (see curve 2 in Fig. 9) was 11.6% 0.85=9.9%.

2.4. Influence of additional internal resonator Fabry-Perot interferometer on the LiF:F_2^- laser generation spectrum

As it was mentioned above to narrow LiF:F_2^- laser radiation spectrum width it is possible to use Fabry-Perot interferometer inside the laser resonator. We inserted additional Fabry-Perot interferometer inside the laser resonator between mirror 4 and 5 (see Fig. 8). New interferometer had base 1.6 mm. Reflectivity of the interferometer mirrors was 70% at wavelength of generation. Substrates for the mirror have wedge with angle 30' and the next surface of the mirror substrate was AR-coated. To separate the interferometer mirrors we implemented three balls for ball bearing because diameters of such type of balls are very close to each other. So it is easy to align an interferometer with these balls. In this case telescope 9, 10 and grating 11 (see Fig. 8) serve to suppress additional transmission peaks of the interferometer. Grating 11 in our experiment has 300 rules per mm, magnification of telescope was about 10^x. Neodymium cw laser radiation pump power was about 15 W.

In Fig. 15 there are interferogram (*a*) and density (*b*) of output radiation of the LiF:F_2^- laser with additional interferometer. Scan area is shown in Fig. 15*a* by white lines. Spectrum width is estimated to be 0.03 – 0.04 cm^{-1}. As it is clear seen from Fig. 3 spectrum consists of two components separated by 0.025 cm^{-1}. This separation corresponds to multiplied to 2 difference of distances mirror 1 – mirror 6 which is equal to 120.8 cm and mirror 6 – mirror – 7 – grating 11 which is equal to 101 cm. This difference is close to 20 cm.

It is worth to mention here that when this difference is close to zero (it is possible to do by moving mirror 6) then spectrum become narrow without additional interferometer but its frequency position becomes highly sensitive to vibrations of the resonator elements and it also depends on angle of active element rotation around its axis. I don't understand the reason of this sensitivity.

Spectrum shape is changed in time and this phenomenon is connected with rotation of LiF active element. In Fig. 15*b* trace 2 shows spectrum for some other interferogram snapshot. Position of spectrum changes less than 0.03 cm^{-1} during 20 minutes. Spectrum was recorded with the help of CCD-camera and videorecorder (JVC HR-J475EE) so it is possible to choose any shot from recording (full time is 20 minutes) after finishing of experiment.

3. Sodium cell, construction, manufacturing and testing.

As it was shown above sodium cell should have temperature at the range 100 - 150 °C. So we made oven for our sodium cell to have this temperature. In Fig. 16 there is draft of the oven. Dimensions of sodium cell are: length 20 cm, diameter 10 mm. Tube of the cell is made from special glass resistant to sodium vapour at this temperature and windows are made from sapphire. There is not any buffer gas inside the cell chamber, only residual gases. A thermocouple is situated nearby the cell surface inside the oven to measure temperature. Outer dimensions of the oven are: length 360 mm, diameter 56 mm. Resistance 2 is nichrome wire that is folded in two. So magnetic field inside the cell due to heating current was minimal. To prevent deposition of sodium atoms on the windows of the cell two additional resistive heater were placed nearby the windows. The coolest place inside the oven where sodium is condensed should be situated far from the windows. So there is done special hole in insulating material and the case of oven nearby of its middle. Sodium vapour pressure in the cell is depends on lowest temperature inside it. We obtained temperature in this place 120 °C. Time of the oven heating is about 2 hours. Supply voltage about 10 V. It is possible to regulate this voltage thus changing the temperature of the cell. Transient time of the temperature is about 1 hour so at this stage of work it is not necessary make special automatic system for temperature stabilisation. It is easy to change temperature manually regulating supply voltage.

Second harmonic of the LiFF_2^- laser at wavelength nearby 589 nm was obtained and this radiation was passed through the cell. Absorption properties of the sodium cell at the sodium resonance wavelength were not tested.

5. Future Directions

Possible ways to improve the LiFF_2^- laser performance.

1. Improvement of spectral selection scheme based on sodium cell as reference wavelength source.

1.1. To develop mechanical control of generation LiFF_2^- laser wavelength driven by computer.

1.2. To investigate experimentally transmission properties of sodium cell at wavelength 589 nm.

1.3. To develop software to monitor generation wavelength of the LiFF_2^- laser.

1.4. To test this software using sodium cell.

2. Rising of output power of the LiFF_2^- laser. To have higher output power in our laser the only is necessary to rise pump power. Estimations show that there are no principal limits from the point of view heat removing from rotating LiF active element at least up to 1 kW of heat power dissipating in the crystal. The only is necessary to choose appropriate dimensions of LiF and rotation speed.

3. Implementation of laser diodes as pump source for the LiFF_2^- laser. Absorption coefficient at wavelength close to 960 nm (maximum of F_2^- cc absorption) is about 4 times more than at 1.064 μm. So there will be the same absorption at 960 nm as at 1.064 μm at lower γ-radiation dose which is used to produce F_2^- cc. So one can expect that pumping of LiFF_2^- at wavelength near 960 nm gives lower losses at wavelength of generation in LiF crystal and higher efficiency.

6. Conclusion

It is suggested to use sodium cell to stabilise generation frequency of the LiFF_2^- laser. It is estimated temperature and stability of temperature and initial transmission of the cell. Scheme of the LiFF_2^- laser with frequency stabilizing system is presented.

It is discussed spectrum width and generation frequency stability that is due to LiF active element rotation and spherical aberrations of telescope elements. Extended 3x3 matrices are implemented for calculation. As calculation shows the laser generation frequency stability it is possible to do better than 0.05 cm^{-1}.

Output power of LiF:F_2^- colour centres laser as function of input power at different reflectivity of mirror 6 (see Fig. 1) was investigated. Slope efficiency 9.9% at narrow (0.1 – 0.2 cm^{-1}) spectrum width was obtained.

Dependence of spectral characteristics of the laser on reflectivity of output mirror was investigated. It was found that the laser spectrum of radiation had shape of narrow (0.1 – 0.2 cm^{-1}) peak and wide (100 – 150 cm^{-1}) background at reflectivity of output mirror less than 40%. Also it was found that ratio of output narrow spectrum power to total power depended on reflectivity of output mirror. Optimum reflectivity of output mirror was found experimentally. For our particular parameters of the laser optimum reflectivity of the mirror was at range 25% - 33%.

Fabry-Perot interferometer with base 1.6 mm and mirror reflectivity 70 % were developed and tested. Spectrum width 0.03 –0.04 cm^{-1} was obtained. Frequency stability better than 0.03 cm^{-1} during 20 minutes was obtained.

Sodium cell and oven for the cell were developed and manufactured.

References

1. W.Happer, G.J.MacDonald, C.E.Max, F.J.Dyson. "Atmospheric-turbulence compensation by resonant optical backscattering from the sodium layer in the upper atmosphere". JOSA - A, v.11, #1, 263 (1994).

2. N.Ilichev. "Laser with Wavelength 0.589 μm ("Sodium Wavelength Laser")". Final report, Contract F61708-97-W0127 (1999).

3. I.S.Grigoriev, G.Z.Meilikhov (Eds.) Handbook of Physical Quantities. CRC, Boca Raton, FL, 1995.

4. G.Megie, J.E.Blamont. "Laser Sounding of atmospheric sodium: interpretation in terms of global atmospheric parameters ", Planet. Space Sci., v.25, 1093 (1977).

5. E.A.Moelwin-Hughes. Physical chemistry. Pergamon Press, London, 1961.

6. A.Gerrard, J.M.Burch. Introduction to matrix methods in optics. John Wiley, New York, 1975.

7. N.Ilichev. "Laser with Wavelength 0.589 μm ("Sodium Wavelength Laser")". First interim report, Project 007021 (ISTC project 1914p) (2001).

8. B.M.Yavorskii, A.A.Detlaf. Handbook on physics. Nauka, Moscow, 1968. (in Russian)

9. Yu.L.Gusev and S.N.Konoplin. Kvant. Elektron., v.8 #6, 1343 (1981). [Sov. J. Quantum Electron. v.11, #6, 808 (1981)].

10. N. N. Il'ichev and P. P. Pashinin. "Narrow-Band Lasing of a Continuous-Wave Laser Using Color Centers in LiF:F_2^- Crystals". Laser Physics, Vol. 11, No. 1, 2001, pp. 112–115.

N.N.Ilichev. "Laser with Wavelength 589 nm ("Sodium Wavelength Laser")". Contract F61775-99-WE039, Final report (2000).

Principal Investigator Nikolay Ilichev

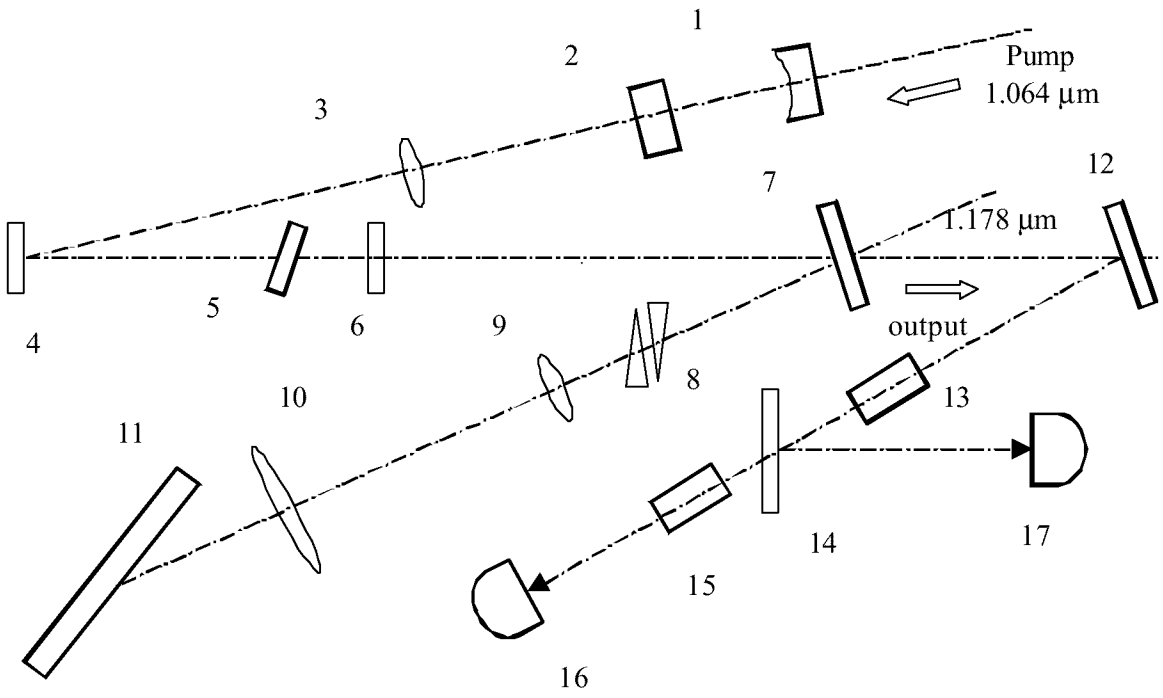

Fig. 1. Principal optical scheme of LiF:F_2^- laser with wavelength tuning.

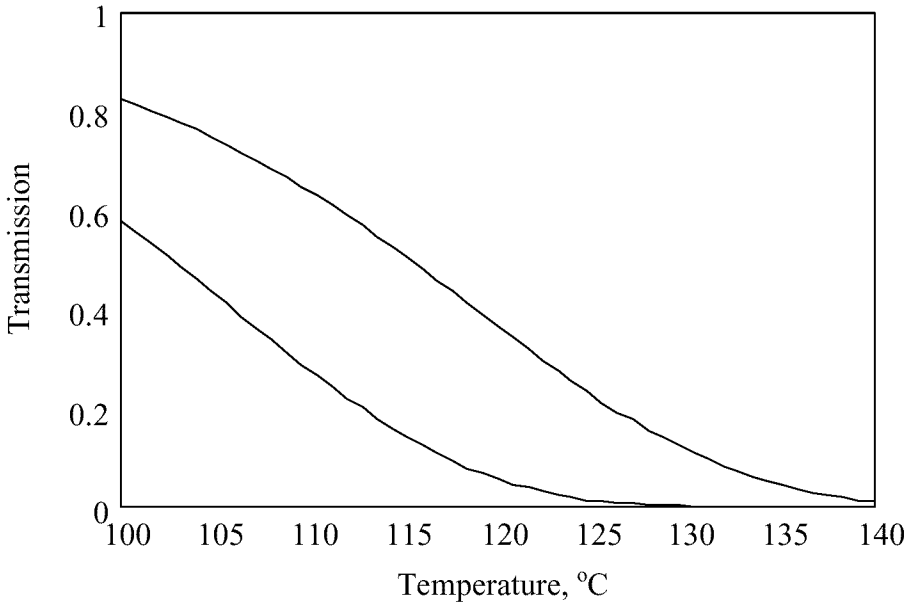

Fig. 2. Transmission of sodium cell vs. temperature. Length of cell is 20 cm. For estimation of temperature range of sodium cell there are plotted two curves for two evaluations of absorption cross section: 1 - $\sigma=3.07\cdot10^{-12}$ cm^2, 2 - $\sigma=8.8\cdot10^{-12}$ cm^2.

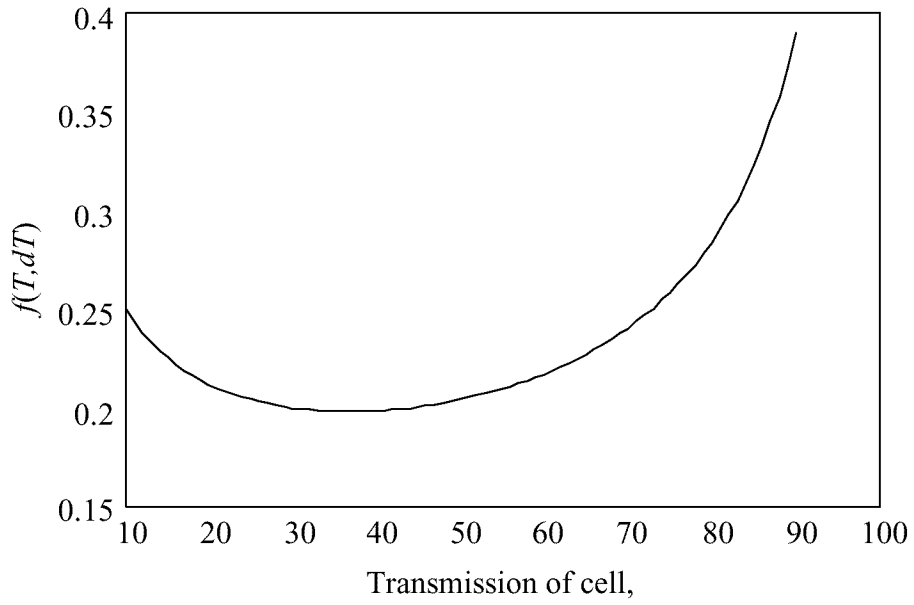

Fig. 3. Accuracy of frequency as function of transmission of sodium cell at the centre of sodium line, δT=1%.

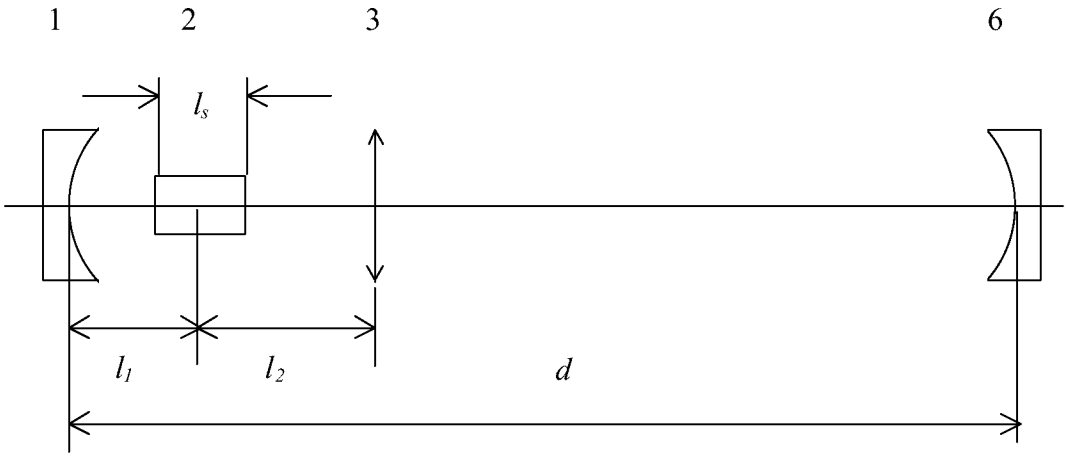

Fig. 4. Scheme where distances inside of LiF:F_2^- colour centres laser resonator are denoted.

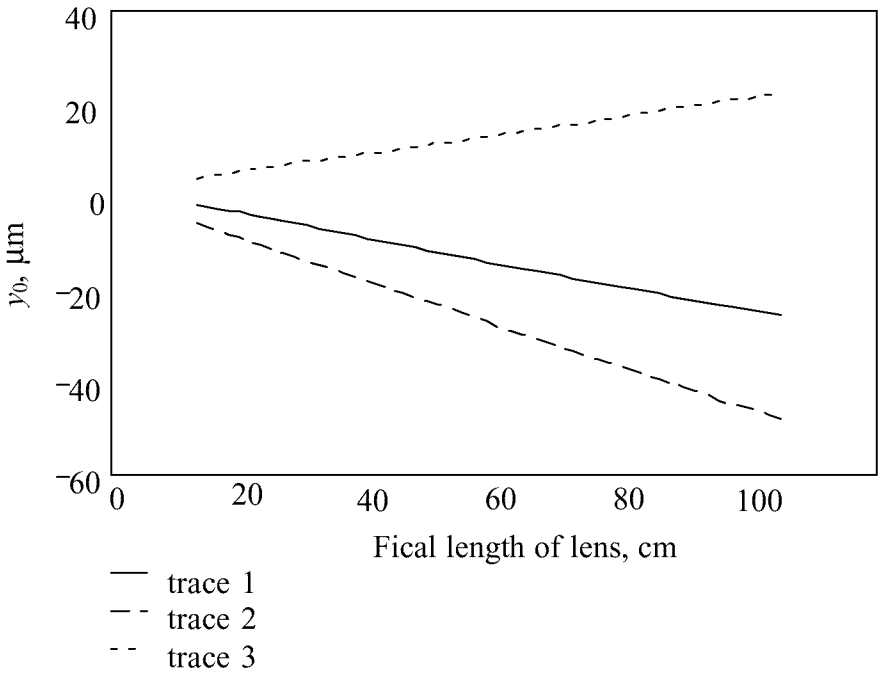

Fig. 5. Position of optical axis at mirror 6 as function of focal length of lens 3 at different angles θ_1 and θ_2. Curve 1 is for $\theta_1=\theta_2=10^{-3}$ rad (tilt of LiF), curve 2 is for $\theta_1=10^{-3}$, $\theta_2=0$ (LiF is a thick optical wedge), and curve 3 is for $\theta_1=0$, $\theta_2=10^{-3}$.

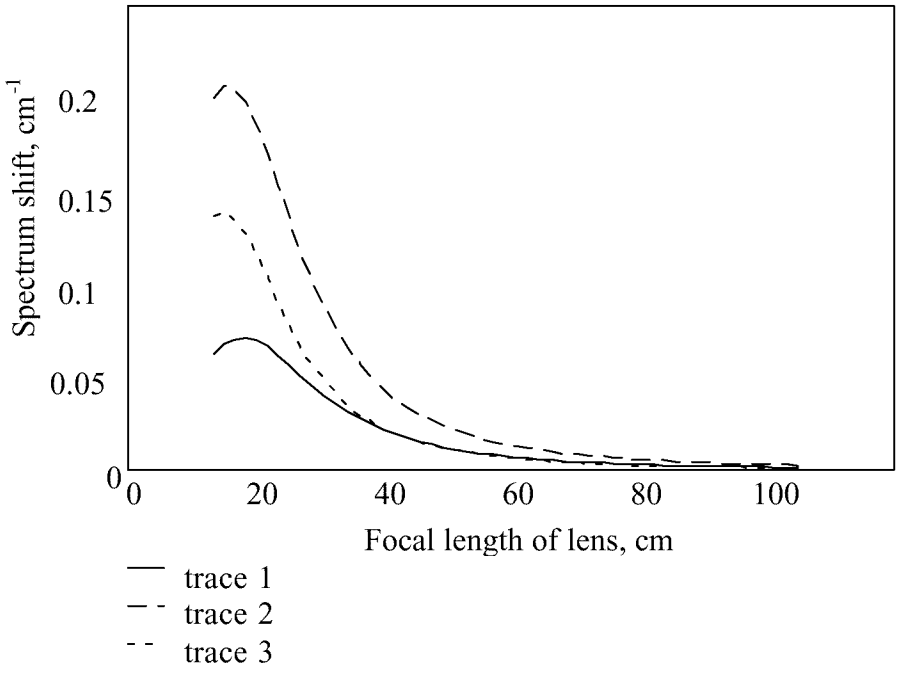

Fig. 6. Calculated shift of generation spectrum as function focal length of lens 3 (Fig. 1) due to rotation of LiF active element. Results presented in Fig. 5 were used in calculation. Curve 1 is for $\theta_1=\theta_2=10^{-3}$ rad (tilt of LiF), curve 2 is for $\theta_1=10^{-3}$, $\theta_2=0$ (LiF is a thick optical wedge), and curve 3 is for $\theta_1=0$, $\theta_2=10^{-3}$. Focal length of lens 10 (Fig. 1) is 60 cm, focal length of eyepiece 9 is 12 cm, grating is 300 groove/mm.

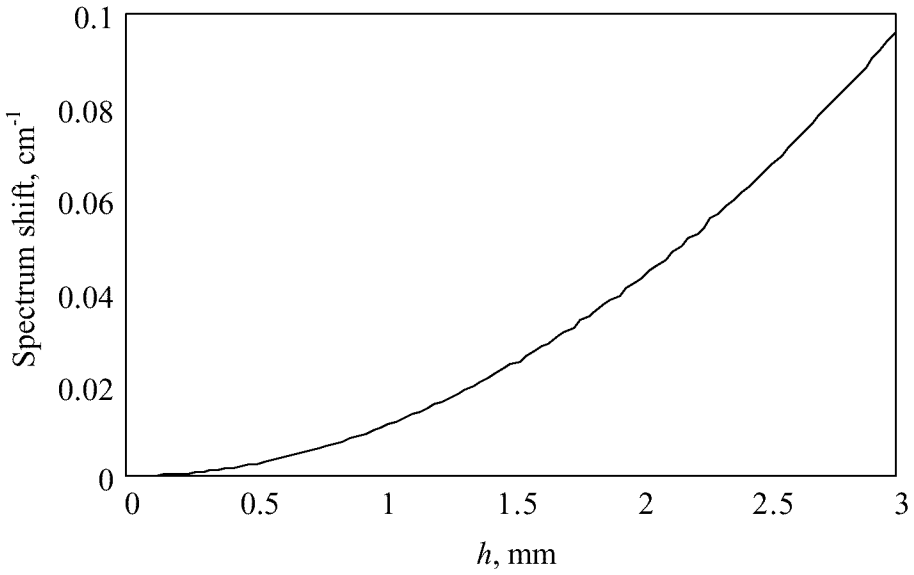

Fig. 7. Calculated shift of generation spectrum as function of transverse optical axis position h at eyepiece of telescope. Is assumed that rotation of LiF active element gives y_0=100 μm.

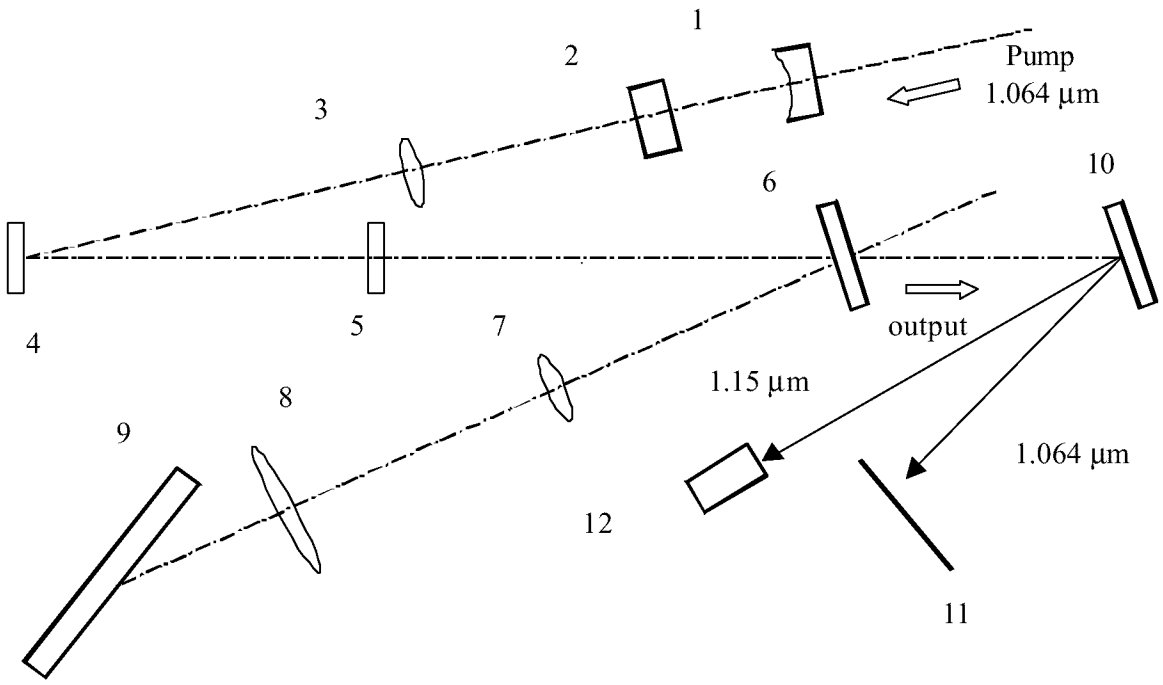

Fig. 8. Experimental setup for measuring parameters of LiF:F_2^- laser with rotating active element.

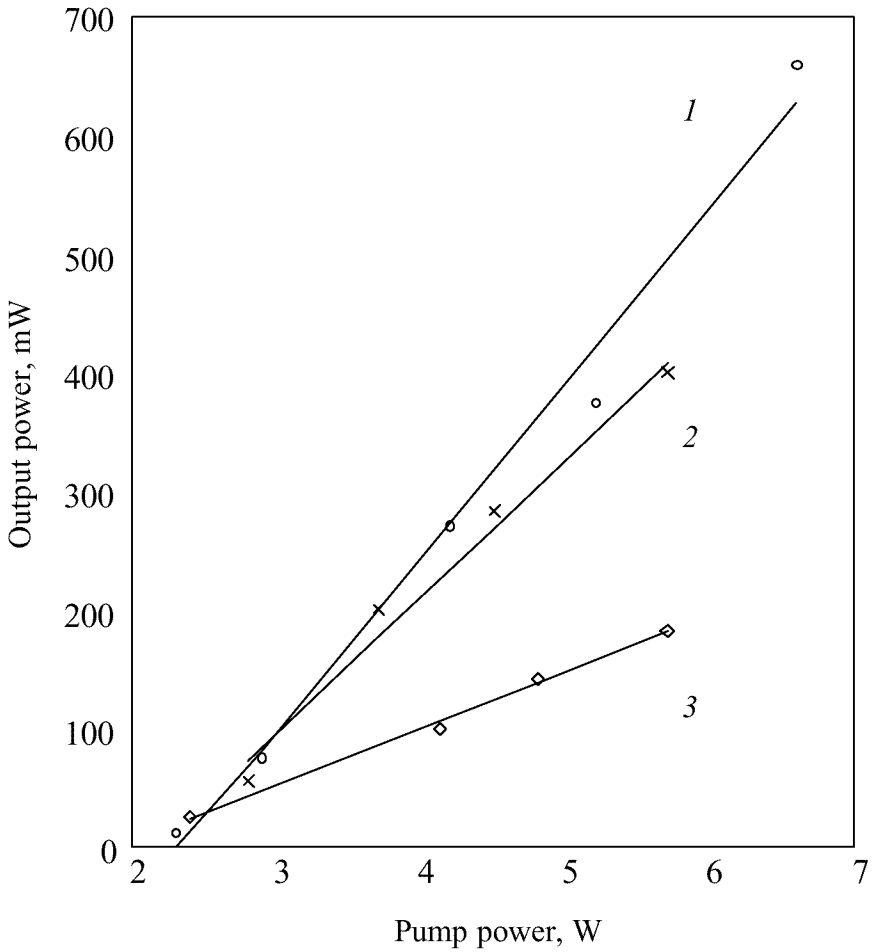

Fig. 9. Output power of LiF:F_2^- laser as function of input power at different reflectivity of mirror 6. 1 - R=0% (mirror 6 is absent), wide spectrum, 2 - R =25%, 3 - R =70%. Slope efficiency 14.8% (curve 1), 11.6% (2), 4.8% (3).

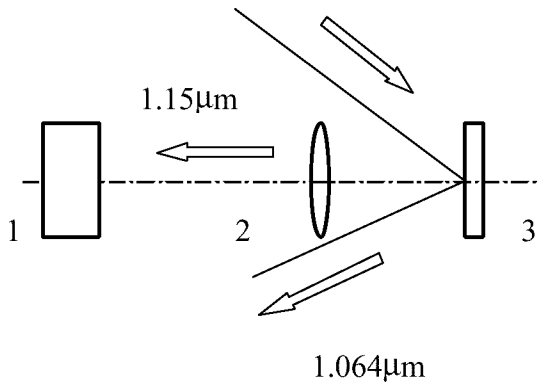

Fig. 10. Scheme of measurement generation spectrum LiF:F_2^- laser. 1 – CCD – camera, 2 – lens with focal length 200 mm, 3 – grating 600 grooves per mm, first order.

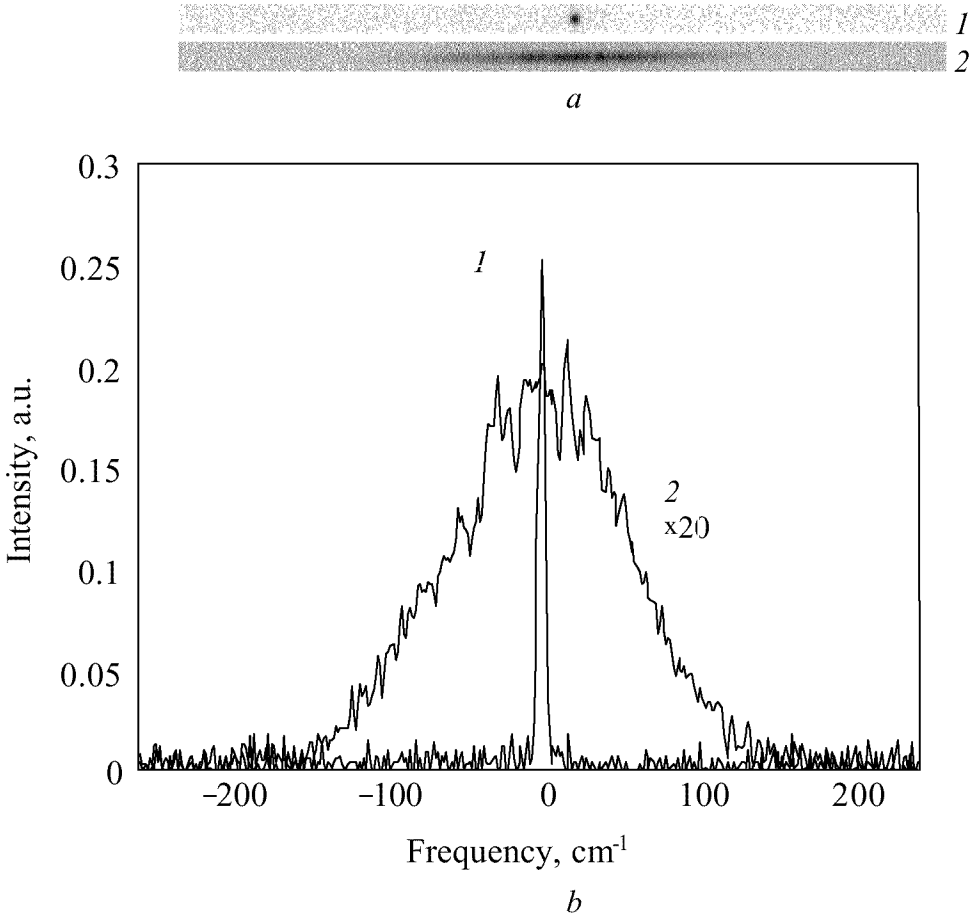

Fig. 11. LiF:F_2^- laser output radiation spectrum *a* – pictures, *b*) - density. 1 – narrow spectrum, 2 – wide spectrum, when there is opaque screen inserted into the laser resonator between mirror 6 (see Fig. 1) and telescope. Reflectivity of mirror 6 is 25 %.
Relative scale for curve 2 is 20 times more than for curve 1.

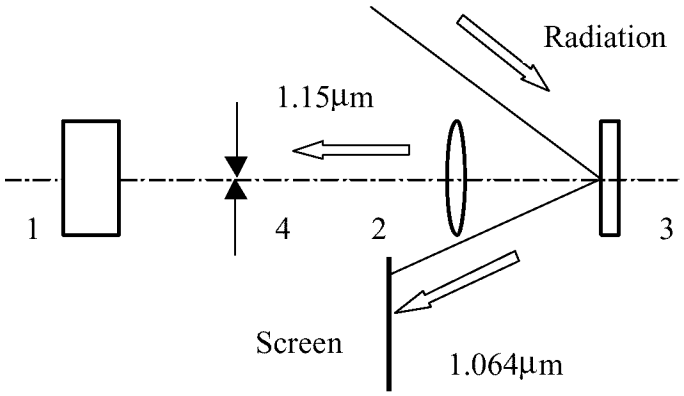

Fig. 12. Scheme of measurement power in narrow and wide spectrum width.

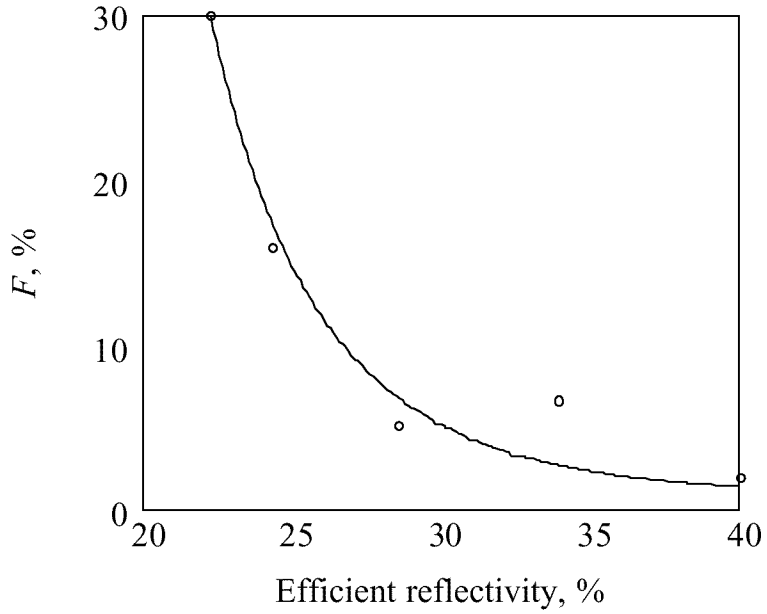

Fig. 13. Dependence of ratio $F=P_w/P_t$ vs efficient reflectivity of mirror 6; P_t - total power and P_w – wide spectrum width power.

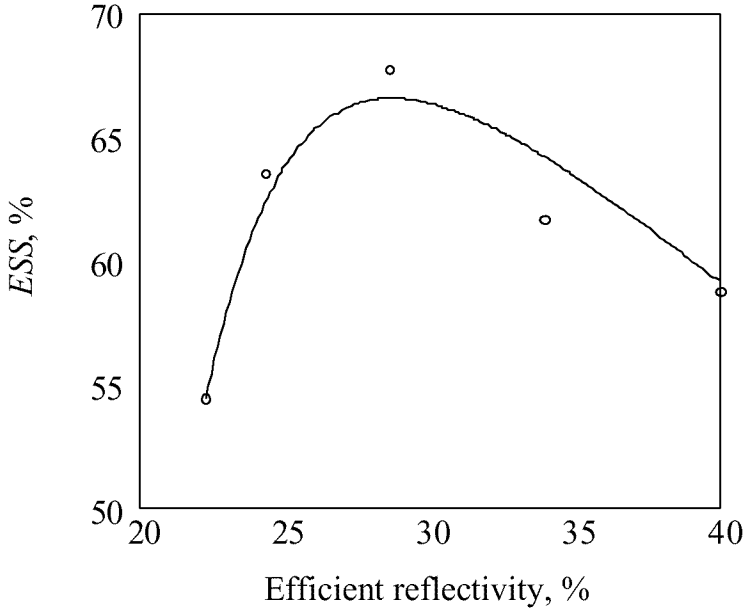

Fig. 14. Efficiency of spectral selection scheme (*ESS*) as function of efficient reflectivity of mirror 6.

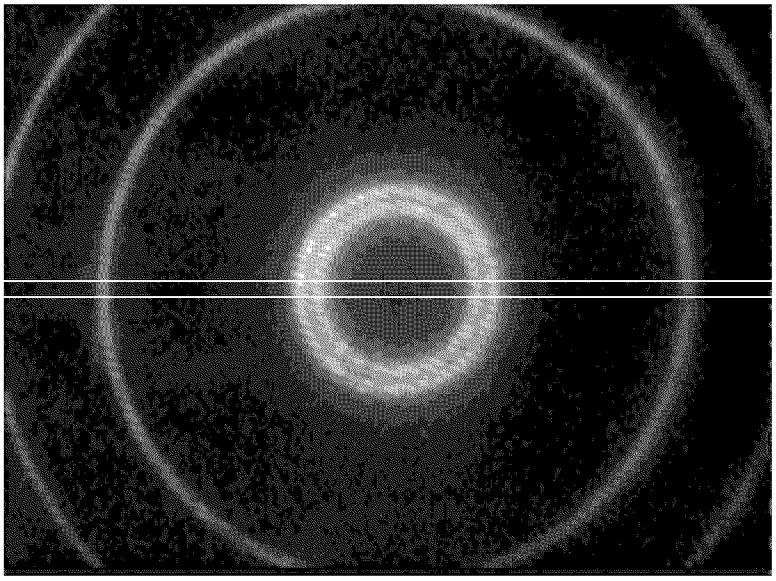

a

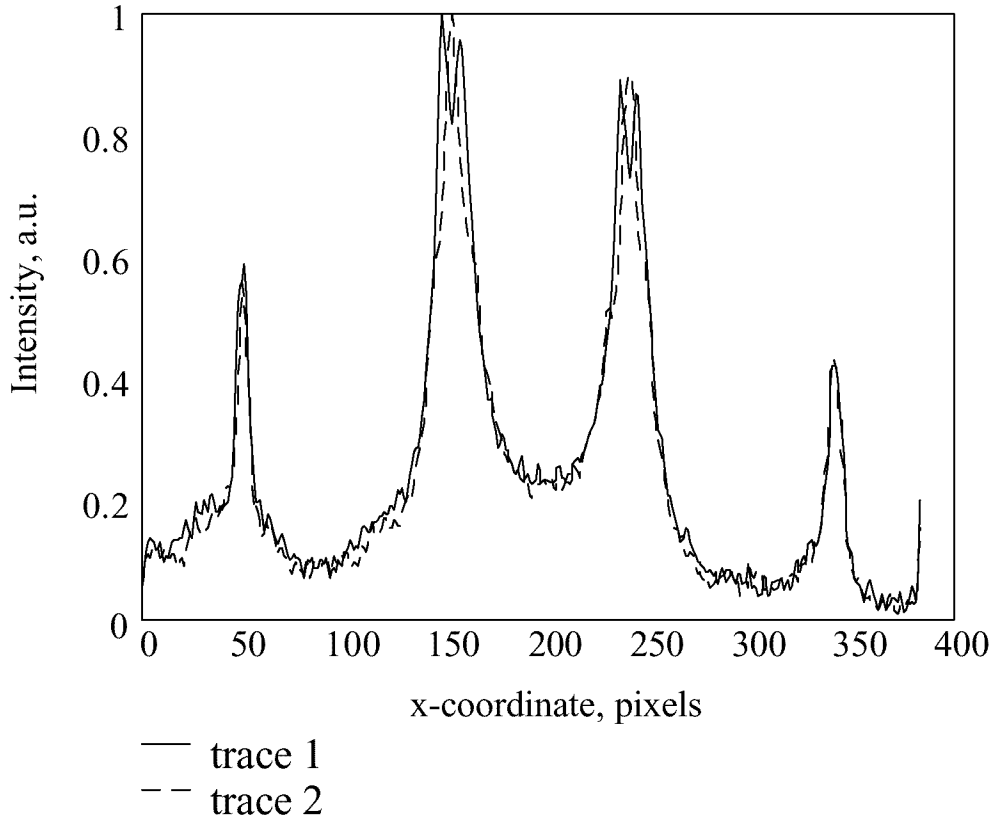

b

Fig. 15. Interferogram (*a*) and density (*b*) of output radiation LiF laser with additional interferometer inside resonator; trace 1 corresponds to (*a*), trace 2 is for some other interferogram as example of spectrum changes due to rotation of LiF. Registration Fabry-Perot interferometer had base 1 cm. White lines in (*a*) restricts scan area.

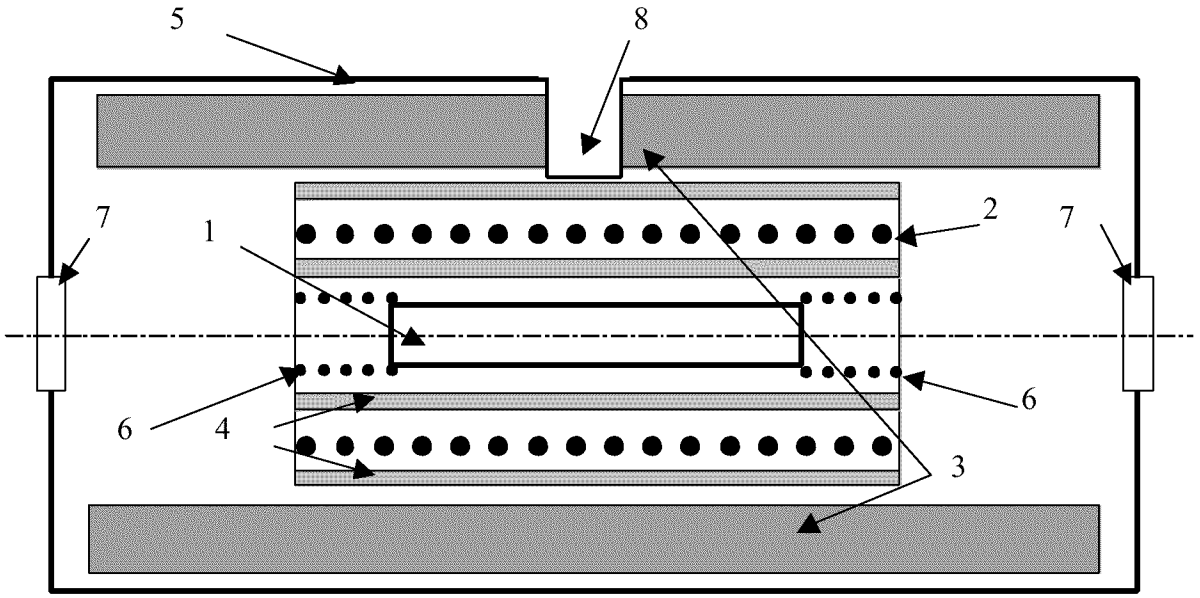

Fig. 16. Principal scheme of sodium cell in oven: 1 is sodium cell, 2 is resistance for heating of oven (6 Ohm), 3 is heat-insulating material, 4 is aluminium tubes, 5 is a case of oven, 6 is two additional resistances for heating of windows of the Na-cell (40 Ohm each), 7 is windows of the oven to prevent air convection, 8 is hole in the oven case and heat-insulating material.

Concurrence with Contract Terms

"The Contractor, General Physics Institute of the Russian Academy of Sciences, hereby declares that, to the best of its knowledge and belief, the technical data delivered herewith Project 007021 (ISTC Project 1914p) "Laser with Wavelength 0.589 μm ("Sodium Wavelength Laser")" is complete, accurate, and complies with all requirements of the contract".

19 December 2001
I.A.Shcherbakov
Corresponding member of RAS, Professor,
Director of General Physics Institute of the Russian Academy of Sciences

---

"I certify that there were no subject inventions to declare as defined in FAR 52.227-13, during the performance of this contract".

19 December 2001
I.A.Shcherbakov
Corresponding member of RAS, Professor,
Director of General Physics Institute of the Russian Academy of Sciences

---